Hindawi
International Journal of Chemical Engineering
Volume 2022, Article ID 6189492, 14 pages
https://doi.org/10.1155/2022/6189492

Research Article

Selenium Migration Mode in Coal Seams: Insights from Multivariate Analysis, Leaching Investigation, and Modelling

Yao Shan,[1] **Yong Qin**,[2] **and Wenfeng Wang**[2]

[1]*School of Emergency Technology & Management, North China Institute of Science and Technology, Langfang 065201, China*
[2]*School of Resource and Earth Science, China University of Mining and Technology, Xuzhou 221116, China*

Correspondence should be addressed to Yao Shan; shanyao@ncist.edu.cn

Received 30 November 2021; Revised 16 March 2022; Accepted 26 March 2022; Published 12 April 2022

Academic Editor: YANQING NIU

Processes controlling selenium concentrations ([Se]) in mine waters were studied at an operating coalmine district in Xuzhou city, China. The geochemistry and mobility of selenium was studied through leaching experiments, multivariate analysis, and numerical modeling. Results showed that selenium leaching was influenced by selenium occurrence in minerals, pH, electron activity (pe), and sulfur concentration in the water. Selenium occurrence in host rock was mainly sulfide minerals, and clay minerals in coal, respectively. Therefore, the oxidation and dissolution of sulfide minerals and transformation of clays may control the release of selenium. Experimental leaching experiments suggested selenium tends to leach more when the solution has more sulfur dissolved. A positive relationship is established between pH and the amount of Se released into solution with four times more Se released at pH 12 compared to pH 2 when leached with high-purity water. This release behavior is higher in O_2-rich environments. The numerical modeling results showed that pH, pe, and sulfur presence in the solution play important roles in selenium adsorption. Selenium was desorbed from adsorbing surfaces under alkaline conditions, specifically when the solution pH was higher than 8. Higher pe values in the solution caused reduced selenium adsorption. In addition, dissolved sulfur competed with selenate for surfaces of adsorption, thus, selenium adsorption decreases as the sulfur concentration increased.

1. Introduction

Selenium is both essential and toxic for animals and humans [1, 2]. The occurrences of diseases caused by deficiency or toxicity of selenium have been reported in New Zealand, USA, Australia, and China [2–9]. In the target area of the present study—Xuzhou-Datun coal mine district, high selenium concentrations in soil (0.21 μg/mg-4.08 μg/mg) and irrigation water have been reported in an earlier study [10]. Considering the low background of selenium level, the high selenium concentrations observed were believed to have come from coal mine water. By the process of weathering, selenium is released from sulfide minerals or organic matters in coal seams [11–15].

In coal mining processes, mineral-water interaction is extremely important as this is the medium of the release of toxic metals which endangers human health and environmental alike. This interaction process includes a series of equilibrium and kinetic reactions, namely oxidation-reduction, dissolution-precipitation, adsorption-desorption, and ion exchange. These processes are governed by water or soil parameters such as pH, redox potential/electron activity (pe), organic matter, mineral composition, soil type, microbial activity, and competing anions [12, 16–18].

In different surrounding environments, trace elements show various behaviors. The typical metal elements have been found to have high concentrations in acid environments [19, 20]. On the other hand, oxyanionic species, like those of certain elements including arsenic (As, AsO_2^-, ... etc.), chromium (Cr, CrO_4^{2-}..., etc.), selenium (Se, SeO_3^{2-}, SeO_4^{2-}... etc.), molybdenum (Mo, MoO_4^{2-}, ... etc.), antimony (Sb, $[Sb(OH)_6]^-$, ... etc.), usually have low concentrations in acid coal mine water, but can be found in relatively high concentrations in alkaline water [12, 21–23].

Besides the release from solid matrix, adsorption also controls the migration of selenium. Selenium can be preferentially adsorbed by different surfaces according to the pH of the solution [24–27]. Furthermore, selenium adsorption

by iron oxides and clay minerals was up to 100% for pH < 8 and declined rapidly when pH increased [24, 26–28]. In addition to the influence of the solution pH, pe also controls selenium adsorption because its valence state changes in different pe environments. Thus, it has been reported that Se (IV) has higher adsorption capacity onto iron-coated sand [29] and stronger adsorption ability than Se (VI) [30–33].

Previous studies have made a lot of successful discussions on selenium migration and adsorption behavior in water. However, there are gaps in the researches and understandings: (1) the experiments of coal and coal ash leaching are usually carried out in an ideal condition, and it is needed to investigate the leaching behaviors in real coal mining environment; (2) although coal and coal ash have been researched thoroughly, the leaching behavior of host rock is seldom studied; (3) in the coal mine water, the selenium concentration is controlled by both dissolution and adsorption; most researches have only focused on one of them; (4) most of the researches have only reported a short-time leaching behavior, a long-term observation is needed to be investigated to demonstrate its full-view leaching behavior.

This study was carried out to explain the high concentrations of selenium in the coal mine water at Xuzhou-Datun coal mine district, although the concentration of this element in the coal seam is low. At the same time, this study is devoted to fill the gap of research and insufficient understanding. In this study, coal and host rock are collected from the active coal mines for the investigation of selenium occurrence and leaching behavior and mechanism. Leaching experiments and modeling were carried out together to investigate migration and adsorption behavior and mechanism on the selenium migration process. As an innovate method, multivariate analysis was used to cluster the elements in solid and liquid samples, then the selenium occurrence and its migration mode could be inferred.

2. Materials and Method

2.1. Study Area. This study was conducted at the Xuzhou-Datun coal mine district located at Xuzhou city, Jiangsu province, eastern China (Figure 1). The hydrogeology unit is encircled by a series of faults (Figure 1), including coal mines named Longdong Sanhejian, and Yaoqiao. Sediment strata in this area are Simian, Cambrian, middle-lower Ordovician, middle-upper Carboniferous, Permian, Jurassic, Cretaceous, Tertiary, and Quaternary system (Figure 2).

The mining seams (No. 7 and No. 9) are embedded in the Shanxi formation, carboniferous system. The Shanxi formation have an average thickness of 116 m, ranging from 62 to 131 m. Gray mudstone, sand-mudstone, and sandstone are the main rocks in Shanxi formation, while some silicon-mudstone and siderite are also present.

Ground water could be found in six aquifers systems, which is shown in Figure 2. Limestone aquifers could be found in the Ordovician system and Taiyuan formation of Carboniferous system, which could be the main sources of the coal seams. Sandstone aquifers could be found in the lower-Shihezi formation and Shanxi formation of Ordovician system. A conglomerate rock aquifer in the Jurassic, and a grit aquifer in the Quaternary are also distributed in the coal mine area.

2.2. Sample Collection and Chemical Analysis. The samples collected for test and leaching experiments include 30 rock/coal samples and 48 water samples. Coal and rock samples were collected from the working area and sealed using plastic bags immediately. The water samples were collected in 1000 ml Nalgene bottles, which were cleaned by 3.2 mol/L HNO_3 and then washed by sample water. A portable JENCO 6010 pH/ORP meter was used to measure pe and pH values.

Major ions and physical parameters of water samples were determined according to Chinese standard in the Jiangsu Provincial Coal Geology Research Institute. Total dissolved solids and hardness were analyzed using the standard GB/T 8538 method. pH was also analyzed in the laboratory using the Glass electrode method (GB/T 6920-86). Mg and Ca were measured using atomic absorption spectrophotometric (GB 11905-89). A quantity of 1000 mg/L of Ca standard solution and 100 mg/L of Mg standard solution was diluted to 0.1, 0.2, 0.5, 1, 2, and 5 mg/L, the standard curve of Ca and Mg were obtained, while fitting the concentrations points of standard solutions minus concentration in blank solution. K and Na were analyzed by flame atomic absorption spectrophotometry (GB 11904-89). A quantity of 1000 mg/L of K and Na standard solution and 100 mg/L of Mg standard solution were diluted to 0.1, 0.2, 0.5, 1, 2, and 5 mg/L. The absorption line of K was set to 766.5 nm and 404.4 nm, and the absorption line of Na was set to 589.0 nm and 330.2 nm. Fe was measured by phenanthroline spectrophotometry (HJ/T 345—2007). Standard Fe solution was obtained by put weighted 0.7020 g of ammonium iron sulfate $(NH_4)_2Fe(SO_4)_2{\cdot}6H_2O$ into 50 ml of 1 : 1 sulfuric acid and then transferred to 1000 mL of volumetric flask. Then the standard solution was diluted to 0.1, 0.2, 0.5, 1, 2, and 5 mg/L to generate standard curve. The wavelength of absorption line of Fe was set to 510 nm. Sulfate and chloride were determined using flame atomic absorption spectrophotometry (GB 13196-91) and silver nitrate titration (GB 11896-89), respectively. The concentrations of the major ions were represented as molality, while the weight concentration was divided by molar mass.

The digestion process was designed in accordance with the earlier studies [34–38]. In the first step of the digestion procedure, 0.05 mg of solid samples were weighted and put into tetrafluoroethylene crucibles, then 3 ml of HNO_3, 1 ml of HF and 1 ml of $HClO_4$ were added and heated until all liquid consumed up. In the second step, the crucible was added 3 ml of HCl and heated to evaporation. In the third step, high-purity water (18 MΩ·cm, Q-Pod Element, Millipore) was used to rinse the crucible three times and then transferred to a 50-mL volumetric flask, dilute with high-purity water to volume. All the acids are analytically pure. All the reagents, including HNO3, HCl, HF, and HClO4, were analytically pure grade, concentrations of which were 68, 38, 40, and 72%, respectively.

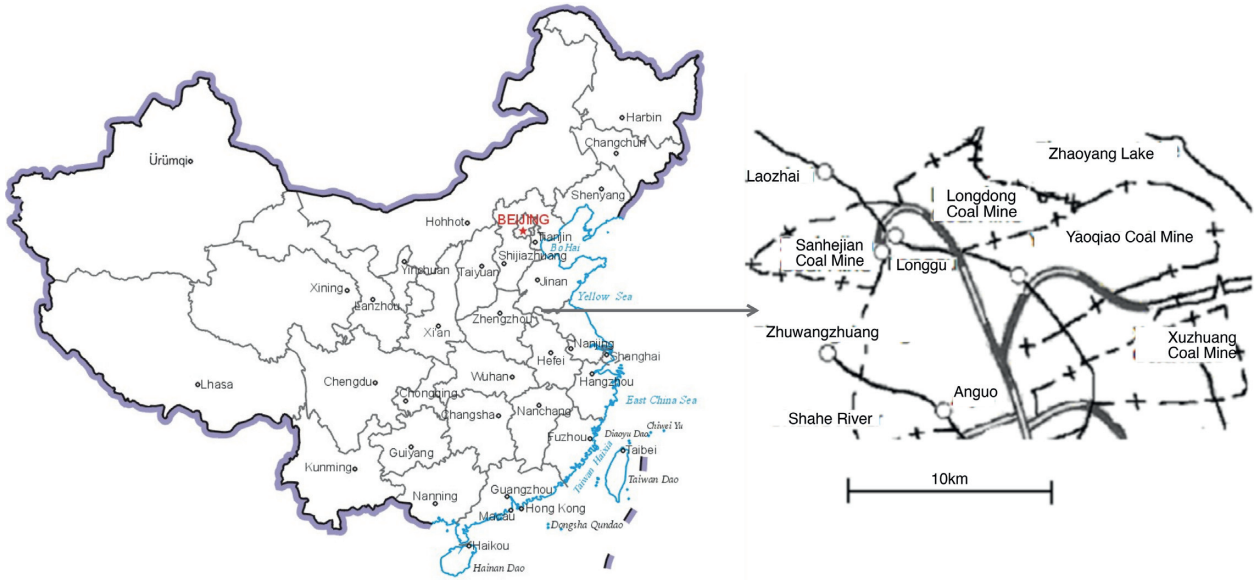

FIGURE 1: Location of the study area. *Note.* The study area is located in the Xuzhou city, Jiangsu province, eastern China. Samples were collected from Sanhejian, Longdong, and Yaoqiao coal mines. Surface water samples were collected from the Zhaoyang Lake which is located to the northeast of the coal mine district.

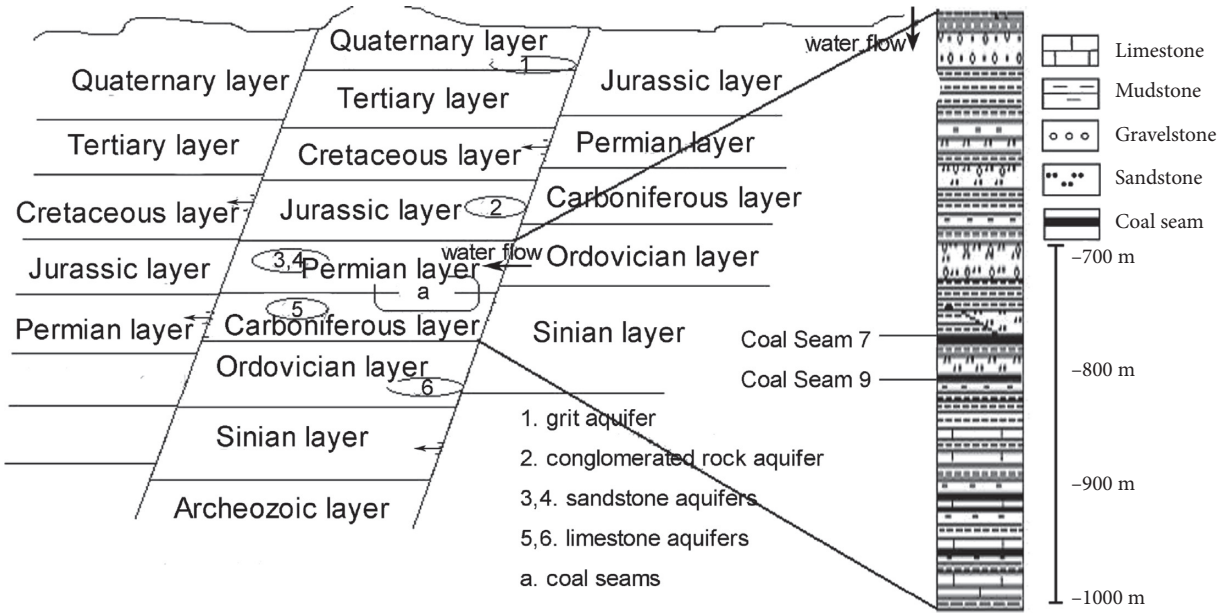

FIGURE 2: Study area with detailed geology and location of aquifers. *Note.* Mined coal seams are located in carboniferous and permian layers. The coal mine water and coal/rock samples were collected from coal seams 7 and 9 which are shown in the geology column. The main aquifer in this district is within the Ordovician layer.

The mineralogy of the coal and rock samples was determined using XRD, which was tested using a Philips PW 1830 diffractometer system with Cu Kα radiation and fitted with a PW 1820 goniometer and a graphite monochromator. The concentrations of trace elements in water/coal/rock samples were determined by ICP-AES and ICP-MS. The ICP-AES analysis was carried out using a JY38S ICP-AES model. The limit of detection and deviation for the analysis carried out by such equipment are 0.01 μg/mL and less than 2%, respectively. The ICP-MS analysis was carried out using the X-Series ICP-MS-Thermo Electron Co., at the following operating conditions: ICP-MS power: 1200 W; auxiliary flow rate: 0.75 L/min, nebulizer flow rate: 0.80 L/min, coolant argon flow rate: 13.50 L/min. An internal standard of Rh was used to determine limit of detection (0.5 pg/mL) and analytical deviation (less than 2%). The ICP-AES and ICP-MS instruments operated routinely. Before each set of testing, standard line for each trace elements was obtained by measuring the standard samples. All the samples were measured twice for its reproducibility.

2.3. Leaching Experiments. The batch mode was used in the leaching experiments to simulate conditions in a coal seam where water movement is slow, following a previous method (with low pO_2; see Stumm and Morgan for details [39]). Closed bottles were used to simulate close environment, and a thermostat which was set to 40°C was used to simulate temperature underground in some experimental sets. The pH and pe values were monitored using a JENCO 6010 pH/ORP meter.

All glassware used in the experiments was previously soaked in 3.2 mol/L HNO_3 for 2 days. Rock/coal samples (Table 1) were ground and sieved to 120 μm. A quantity of 30 mg of solid sample and 1000 mL aliquot of high-purity water with initial pH values of 2, 5.6, 7, and 12 were used in each experimental set. Leachate solutions were collected using syringes at 2, 6, 24, and 48 h, some experiments lasted for up to 10 days. A quantity of 0.5 mol/L HNO3 was added into all collected samples. Selenium concentrations in collected sample are given in Table 2.

In addition to leaching experiments, water samples including those collected from the Zhaoyang and Yunlong Lakes (Figure 1) were shaken every 2 hours for up to 10 days at 40°C. Results are given in Table 3.

2.4. Multivariate Analysis. The solid samples are composed of minerals and elements, and the liquid samples are composed of ions and trace elements. Concentrations and coexisting behaviors of trace elements suggest the occurrence and leaching mechanisms during the water-rock interaction. As the sample-concentration pattern is a matrix-like system, the technology of the multivariate analysis can be used to identify the different and similar components, which usually suggest different occurrence in solids, and immigration mechanism in waters.

To understand the selenium occurrence in coal and host rock, we applied the method of principal component analysis (PCA) with R language. The data are first standardized using the original data matrix, then divided every value with each column by the column standard deviation. The orthogonal principals are then rotated to achieve the maximum deviation. After PCA, the matrix is reduced to two or three smaller ones that consist of PC loadings and PC scores. In our study, the PC loading means the values that every element have on principal components, and the PC scores means the values every sample have on principal components. The PC loadings suggest similar behavior of elements occurrence in rock and coal matrix, and the PC scores suggest the samples with similar composition.

2.5. Geochemical Modeling. Besides the experimental work to characterize the behavior of leaching selenium in the water-rock/water-coal interaction at Xuzhou-Datun coal mine district, this was also modeled using the following aqueous geochemistry software: PHREEQC (version 2.15.05), Geochemist' Workbench (GWB version 7.0) and MINTEQ (version 2.53). Database Wateq4f.dat were used while modeling using PHREEQC and MINTEQ.

Two dominant processes controlling selenium distribution were modeled: after dissolution-precipitation and adsorption onto iron oxides and hydroxylated silicates.

Modelling consisted of three parts at varying experimental conditions. First, species of Se were calculated; then the adsorption of Se species onto selected surfaces was simulated; and finally, the interaction of the water-rock/coal—assuming equilibrium—was modeled under closed and open conditions.

The speciation of selenium was modeled using the GWB software; assuming a solution volume of 1000 ml with ionic strength of 0.1 mol/L (this last assumption was made based on the analytical results obtained from the Sanhejian coalmine water samples). Se in the coal mine water was set to 6 nmol/L. Other major ions were limited to concentrations found in the water from the Sanhejian coal mine, shown in Table 3. Surface water in the table stands for the water samples that were collected from surface water in the coal mine district, the carbonate-seam water means the water samples that were collected from carbonate seams from the coal mine district, and the coal mine water means the water samples that were collected from coal mines underground. The system temperature was kept at 40°C, same as the coal mine environment.

Both, the adsorption of selenium species, including selenite and selenate and adsorption competition by sulfate were modeled using the PHREEQC and MINTEQ programs. The adsorption model used was the Diffuse Layer/Surface Complexation model (DL/SC) as suggested in [40, 41] and coded in PHREEQC and MINTEQ. The adsorbent was set to be amorphous iron oxides, also called ferrihydrite (HFO). This assumption was based on the fact that although selenium can be adsorbed by iron oxide, clay, carbonate, pyrite, etc., it has both a greater adsorption capacity than clay minerals and a better ability to adsorb trace elements [42]. Thus, the HFO was used to represent adsorbents. The specific surface of the HFO was assumed to be 600 m^2/g as recommended [40], of this $2.24e-3$ mol/g and $5.6e-5$ mol/g were considered to be weak and strong sites, respectively.

pe, pH, and some major ions concentrations were varied during modeling. Changes in pe combined with air phase were used to simulate "closed" and "open" system behavior. Thus, equilibrium with the air phase meant an open environment, while no air phase signified a closed system. Modeling results showed that open system had a high pe-in the range of 10–15; this meant that selenium adsorption was likely to be impacted by water parameters. In closed system, pe varied from 0 to 4.

The system pH was controlled by hypothetical additions of NaOH in the modeling; at the beginning of the model, running pH was set to zero, then as modeling time evolved, NaOH was "added" to increase the pH of the system. During every step, the system was allowed to achieve equilibrium after that PHREEQC was used to calculate the adsorption ratio of selenium.

To find out the impact of ions at different concentrations on the adsorption of selenium species, two sets of

Table 1: Mineralogy and composition of the coal seam rock at the Xuzhou-Datun coal mine district.

Samples name	Quartz	Pyrite	Feldspar	Albite	Illite	Kaolinite
Sanhejian roof (S1)	52%	Trace	1%	<1%	17%	28%
Sanhejian floor (S2)	85%	—	—	<1%	6%	7%
Yaoqiao roof (Y1)	36%	2%	—	—	4%	56%
Yaoqiao floor (Y2)	62%	—	1%	—	15%	20%
Composition	SiO_2	FeS_2	*Composition*	K_2O/Na_2O	Al_2O_3	SiO_2
Quartz	100%	—	Feldspar	16.9% K_2O	18.3%	64.7%
Pyrite	—	100%	Albite	11.8% Na_2O	19.5%	68.7%
Composition	K_2O	MgO	Al_2O_3	SiO_2	H_2O	
Kaolinite	—	—	39.5%	46.5%	14.0%	
Illite	7.4%	2.6%	30.6%	54.8%	4.7%	

Table 2: Selenium concentrations in the collected rock/coal samples.

Set of experiments	1: rock; deionized water; open			2: rock; deionized water		3: rock; surface water; open	
Initial pH	2	5.6	12	5.6; open	5.6; closed	8.69	8.53
0 hr (μmol/L)	0.000	0.000	0.000	0.000	0.000	0.047	0.097
2 hrs (μmol/L)	0.013	0.026	0.049	0.026	0.016	0.058	0.074
6 hrs (μmol/L)	0.022	0.033	0.077	0.033	0.035	0.067	0.081
24 hrs (μmol/L)	0.034	0.059	0.013	0.059	0.051	0.077	0.106
48 hrs (μmol/L)	0.039	0.080	0.154	0.080	0.063	0.090	0.133

Table 3: Physicochemical parameters and concentration of major ions and selenium in water samples from the Xuzhou-Datun coal mine district.

Type of samples	Surface water		Carbonate-seam water		Coal mine water					
Collected from	Yunlong lake	Zhaoyang lake	Sanhejian coal mine	Sanhejian coal mine	Longdong coal mine	Yaoqiao coal mine	Sanhejian coal mine	Sanhejian coal mine	Sanhejian coal mine	Sanhejian coal mine
K + Na (mmol/L)	0.786	4.944	19.572	21.432	13.855	56.90	60.97	30.467	27.049	40.860
Ca (mmol/L)	1.055	1.701	14.87	15.51	11.606	0.8148	1.732	17.955	22.518	6.944
Mg (mmol/L)	0.689	1.945	7.308	7.335	8.829	1.699	1.184	9.821	11.706	4.464
Cl (mmol/L)	1.220	4.395	12.99	14.11	6.882	10.99	19.04	13.434	12.839	17.451
SO_4^{2-} (mmol/L)	0.849	1.994	24.35	25.47	24.903	24.35	20.67	41.185	45.110	31.382
HCO_3^- (mmol/L)	1.356	3.853	2.238	2.072	3.120	2.238	6.422	2.958	3.161	3.363
CO_3^{2-} (mmol/L)	0.290	0.622	0.207	0.289	0	0.663	0.290	0.648	0.162	0
NO_3^- (mmol/L)	—	—	—	—	0.002	—	—	0.020	0.003	0.073
Hardness (mg/L)	175	362	2208	2274	1023	249	290	1390	1713	571
TDS (mg/L)	302	848	4167	4376	2300	4206	4569	3940	4122	3518
pH	8.69	8.53	8.10	8.15	7.80	8.56	8.15	8.00	7.90	7.85
Ionic strength (mmol/kg)	15.6	24.6	109.1	113.2	57.9	64.9	68.2	92.6	74.0	101.7
Se (nmol/L)	0.0536	0.11	0.157	0.19	0.759	0.355	0.196	0.683	0.819	0.62

concentrations of dissolved major ions were used in the modeling: high-purity water and coal mine water composition.

The initial settings simulated 0.6 nmol of selenium added to 1000 ml of high-purity water containing 0.1 g HFO of adsorbent. The following assumptions were taken:

(a) The coal seam system is closed before mining, thus it is isolated from oxygen and any organic rich waters

(b) The coal seam system is open during mining, then it exposed to oxygen

(c) The redox potential of water surrounding the coal seam changes at open system conditions

(d) Selenium will change among its four oxidation states depending on the pH and pe conditions

(e) The dominant selenium species are H_2Se and HSe^- and Se precipitates under closed system conditions

(f) The concentration of dissolved selenium in the coal mine water is controlled through adsorption [28] rather than precipitation [21] processes

(g) Iron minerals are the most important media for Se adsorption

(h) The chemistry of iron mineral is highly influenced by pH and pe conditions

(i) The dominant iron mineral in the coal bearing seam at closed system is pyrite, this however will oxidize, dissolve, and reprecipitate as iron oxide and iron hydroxide minerals such as hematite and goethite when the coal bearing seam is at open conditions

3. Results and Discussion

3.1. Field Observation. Table 3 gives the concentration of major cations and anions, total dissolved solids (TDS), pH, ionic strength and [Se] in surface, carbonate seam, coal mine water, and surface water samples. Carbonate seam, as well as coal mine water samples have higher values of ionic strength, hardness, and TDS than surface water. Alternatively, pH and Eh values remained constant for all types of waters, an average of 8.5 and 220 mV, respectively—as measured in field. The carbonate-seam water and surface water have significant higher concentrations of Ca^{2+} and Mg^{2+} than the surface water. The coal mine water has the highest K^++Na^+/Ca^{2+} ratio. The concentrations of Cl^- and SO_4^{2-} are similar for both carbonate seam and coal mine waters, but lower for surface water. The concentrations of CO_3^{2-} and NO_3^- are usually low in carbonate seam water but vary for the other two types of waters.

The concentration of selenium in coalmine water is the highest of the three types of water under study; this value exceeds the Chinese standard limits for ground and surface waters if destined for drinking water purposes; 0.127 nmol/L and 0.253 nmol/L, respectively. It is also higher than the standard limit—independently of the origin—for irrigation; 0.253 nmol/L. [Se] in the coal mine water is about 0.2–0.9 nmol/L, this implies that this water needs to be treated before being used for either drinking or irrigation purposes. As the coal mine water was discharged into surface water, selenium concentration may be lowered due to adsorption. However, we compared the selenium concentration in surface water both from the coal mine district and non coal-mine district of Xuzhou-Datun area. According to our observation, the selenium concentration in coal mine district surface water was higher (0.11 nmol/L) than that of noncoal mine district surface water (0.0536 nmol/L). Huang et al. [10] reported that the selenium concentration in irrigation water in the Xuzhou area was from 0.03 to 3.67 nmol/L with a medial value of 0.63 nmol/L which is comparable with our research. At the same time, soil in the Xuzhou area was found to be contaminated by selenium. The results suggested that the selenium in coal mine water is an important source of surface water.

3.2. Rock Composition, Selenium Occurrence, and Its Influence on Selenium Leaching. The coal host mineralogy, determined by XRD, is shown in Table 1. As seen, quartz and kaolinite are the main minerals in the coal seam host rock, with the former being the most abundant—52–85%—in three of four locations sampled; only in the roof of the Yaoqiao mine, kaolinite was the most abundant mineral—53%. Because of the low mineral proportion, mineralogy in the coal was not quantified.

The relationship of elements in rock and coal samples was calculated by using PCA method. For the rock samples, two PCs were selected based on the screen test, which explained 63% (34% and 29%, respectively) of all deviation, the PC loading is shown in Table 4. The PCA result was clustered using GMM algorithm (shown in the Figure 3(a)), in which the group one includes Zn, Ba, Mn, Fe, Mg, As, Hg, Se, Cd, represented by hollow squares, and the group two includes Mo, Pb, Cr, V, Cu, Ti, Sr, Ca, Al, represented by solid circles, respectively. Considering the element combination behavior and previous studies [43–46], the RC1 stand for sulfide minerals, especially pyrite. Therefore, selenium is mainly occurring in coal host rock as pyrite.

For the coal samples, also two PCs were selected based on the screen test, which explained 69% (45%, 24%, respectively) of all deviations; the PC loading is shown in Table 5. The PCA result was clustered using GMM algorithm (shown in the Figure 3(b)), in which the group one includes Mo, Pb, Cr, V, Cu, Ti, Al, As, Hg, Se, represented by solid circles, the group two includes Zn, Fe, Cd, represented by hollow squares, the group three includes Ba, Mn, Sr, Mg, Ca, represented by solid triangles, respectively. Considering the element combination behavior and previous studies [15, 47, 48], the RC1 stands for clay minerals. Therefore, it is concluded that selenium is mainly occurring in coal as clay minerals.

The roof rock has more pyrite than the floor rock in the samples of both mines; this is relevant because sulfides, such as pyrites, may be carriers of selenium in coal and coal seam host rocks, where they are either replaced by some other elements (such as sulfur) or as selenium minerals. Before and after leaching experiments, illite tends to transform to kaoline, and albite and pyrite tend to consume. Therefore, the transformation and dissolution are important mechanism of selenium release. In host rock, the oxidation and dissolution should be the key mechanism of selenium release, and the transformation of clay mineral should be the key mechanism in coal.

In case of sulfite occurrence, selenium would be stable under anaerobic conditions, and dissolve in an oxygen-rich environment. In case of clay occurrence, selenium may be released during the water-rock interaction, especially in an oxygen-rich environment.

Table 4: Loadings of PCA of the roof samples.

	RC1	RC2
Mo	0.09	0.89
Zn	0.68	−0.14
Pb	−0.40	0.68
Ba	0.76	−0.05
Mn	0.71	−0.07
Cr	0.04	0.69
V	−0.22	0.09
Cu	−0.43	−0.30
Ti	−0.26	0.59
Sr	−0.01	−0.71
Fe	0.74	−0.51
Mg	0.73	−0.51
Ca	−0.06	−0.69
Al	−0.19	0.93
As	0.73	0.63
Hg	0.86	0.40
Se	0.95	0.06
Cd	0.95	−0.08

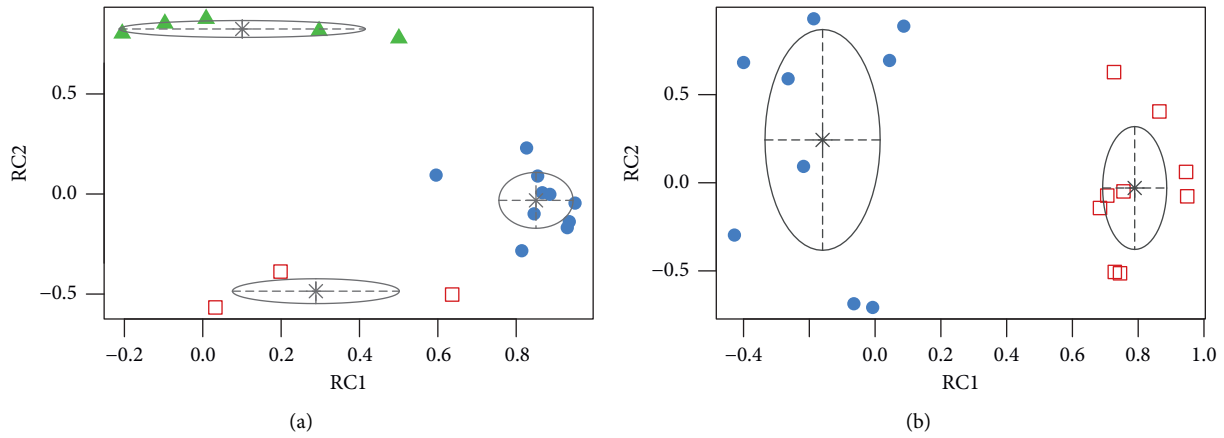

Figure 3: PCA and clustering results of elements in rock (a) and coal (b). *Note.* Features of the element contents in rock and coal were reduced by PCA method and then clustered using GMM algorithm, shown in (a) for rock and (b) for coal, respectively. In (a), the elements were clustered into two groups, the group one includes Zn, Ba, Mn, Fe, Mg, As, Hg, Se, Cd, represented by hollow squares, the group two includes Mo, Pb, Cr, V, Cu, Ti, Sr, Ca, Al, represented by solid circles, respectively. In (b), the elements were clustered into three groups, the group one includes Mo, Pb, Cr, V, Cu, Ti, Al, As, Hg, Se, represented by solid circles, the group two includes Zn, Fe, Cd, represented by hollow squares, the group three includes Ba, Mn, Sr, Mg, Ca, represented by solid triangles, respectively.

To illustrate the effect of anaerobic and oxygen-rich conditions on the dissolution of selenium minerals in the coal mines under study, the speciation modeling of selenium in coal mine water was carried out; results are given in Figure 4. The gray area delimits the typical conditions of pH and pe for the coal mine water. As seen, SeO_3^{2-} and SeO_4^{2-} are the main species in that region. If the pH of coal mine water is below 7, the main species would be $HSeO_3^-$. In an aerobic environment, SeO_4^{2-} will be more abundant than SeO_3^{2-}.

3.3. Selenium Leaching Behavior and Mechanism. The geochemistry and mobility of selenium in coal mine water were studied using leaching of coal seam samples with both surface water and high-purity water, at three groups of different conditions; results are shown in Figure 5.

In the first group—Figure 5(a), host rock samples were leached with high-purity water in an open-system arrangement with varying pH from an initial value of 2–5.6, and finally 12. The second group (Figure 5(b)) compared the behavior of host rock samples being leached with high-purity water at ph 5.6, under open- and closed-system conditions. The third group—Figure 5(c)—consisted of leaching host rock samples with two types of surface water under an open environment, the first surface water had an ionic strength of 24.6 mmol/L and sulfur content of 1.994 mmol/L, while the second had an ionic strength of 15.6 mmol/L and a sulfur content of 0.849 mmol/L.

3.3.1. pH and Pe Influences on Selenium Leaching and Adsorption. The pH and pe may influence the selenium leaching in two ways. First, the selenium-contained minerals

Table 5: Loadings of PCA of the coal samples.

	RC1	RC2
Mo	0.83	0.23
Zn	0.03	−0.57
Pb	0.93	−0.17
Ba	0.50	0.78
Mn	−0.10	0.85
Cr	0.85	−0.10
V	0.81	−0.28
Cu	0.85	0.09
Ti	0.87	0.01
Sr	0.01	0.88
Fe.	0.64	−0.50
Mg.	0.30	0.82
Ca.	−0.21	0.80
Al.	0.95	−0.05
As	0.60	0.09
Hg	0.89	0.00
Se	0.94	−0.14
Cd	0.20	−0.39

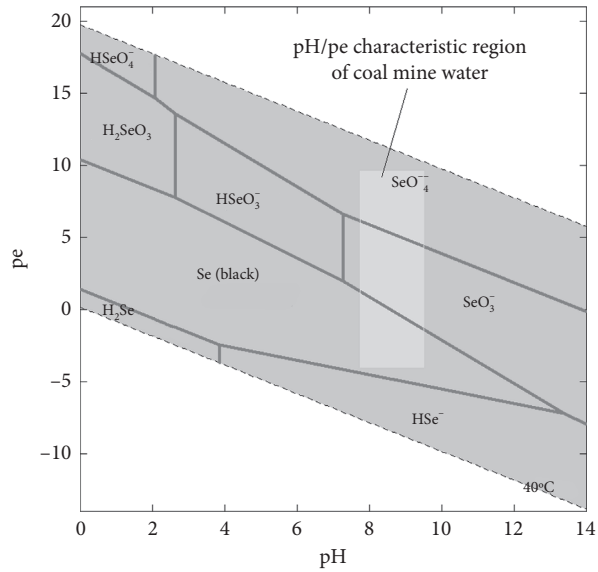

Figure 4: pH-pe diagram of selenium species. *Note.* Two assumptions were taken to build this diagram; the first is that [Se] in the coal mine water was 0.6 nmol/L, while the second is that temperature was 40°C which is same as the temperature underground.

release selenium varies in different pH and pe values [49]; second, the selenium in water is adsorbed by adsorbent differently with change of pH and pe values [18]. It was observed that pH and pe varied during the coal leaching experiments. In an open environment, after 48 hours, the solution pH of the three experimental sets changed from 2, 5.6, and 12 to 2.42, 7.65, and 10.09, respectively. The pe values of 6.75, 3.93, and 1.63 did not vary significantly.

As mentioned previously, the pH of the solution controls the leaching behavior of selenium; this effect is clearly depicted in Figure 5(a). As seen, when using high-purity water of pH 2 to leach host rock samples, the [Se]—after 48 hours—is 0.0386 nmol/L in the resulting solution. When using high-purity water of pH 5.6 and 12, [Se] resulted in 0.0796 and 0.154 nmol/L; respectively. Thus, it can be concluded that selenium is likely to be released as pH increases.

Similar results to the abovementioned were reported by Iwashita et al. [23]. They researched the leaching of Coal Fly Ash (CFA) and found that the selenium leaching was pH-dependent. When the pH solution was under 6, less than 20% selenium leached, while up to 50% leached when the pH solution was over 10.

Canty and Everett [50] also reported the influence of pH on selenium leaching in coal. They studied the leaching of fluidized bed combustion ash injected into abandoned coal mines. After 24 hours of contact of water with the ash, both the leached solution alkalinity and pH gradually increased, the concentration of metals such as Al, Zn, and Ni decreased, but the concentration of Se was well above the criteria for continuous and maximum concentration levels [51–55].

Figure 6 shows the modeling results of adsorption of selenium at open and closed system with varying pH from 1 to 12. As seen for the open-system case—with pe above 10—selenium is almost 100% adsorbed in the pH region 2 to 6, outside such that the Se adsorption sharply reduced. Similar results were obtained for the closed system—with pe around zero—the only difference was that the pH region affecting Se adsorption was larger covering values from 2 to 8. These results show that in open as well as in closed systems, selenium adsorption was in inverse relation to pH.

The modeling results are comparable to those obtained by leaching experiments in this research and to previous studies. For example, You et al. [32] reported that the SeO_3^{2-} adsorption on hydroxides with double layer of Mg-Al and Zn-Al declined when pH was above 10 and below 4.5. El-Shafey [28] found that SeO_3^{2-} adsorption had a peak ratio when pH was equal to 6 and decreased when pH was above 8. Modelling and laboratory results in this study suggest that selenium adsorption from the coal mine water onto the present surfaces will be high at the typical range (7.5–9) found in the mine waters at the coal mines in Xuzhou area, China.

Experiments in this study also showed that selenium concentration in the leached solution increased with pe. After 48 hours of leaching host rock samples with high-purity water (initial pH was 5.6), the concentration of selenium in the leached solution was 0.0796 and 0.0634 nmol/L, under open- and closed-system regimes, respectively. The pe values were 3.93 for the former and 2.68 for the latter. Schwartz et al. [31] studied the selenium leaching behavior from coal ash, and it is found that [Se] increased sharply and then decreased. Under the aerobic condition, the [Se] increased to 53 μg/L at 24 h and decreased to 29 μg/L at 2 weeks. Meanwhile, the [Se] increased to 94 μg/L at 4 h and decreased to 1.8 μg/L at 2 weeks under the anaerobic condition.

Modeling results also showed that pe had a high impact on selenium adsorption, as seen in Figure 7. This shows the modeling at varying pe from −2.5 to 13.5 and constant pH of 7. Under such conditions, the selenium adsorption ratio on HFO was reduced from nearly 100% to 0. Thus, selenium

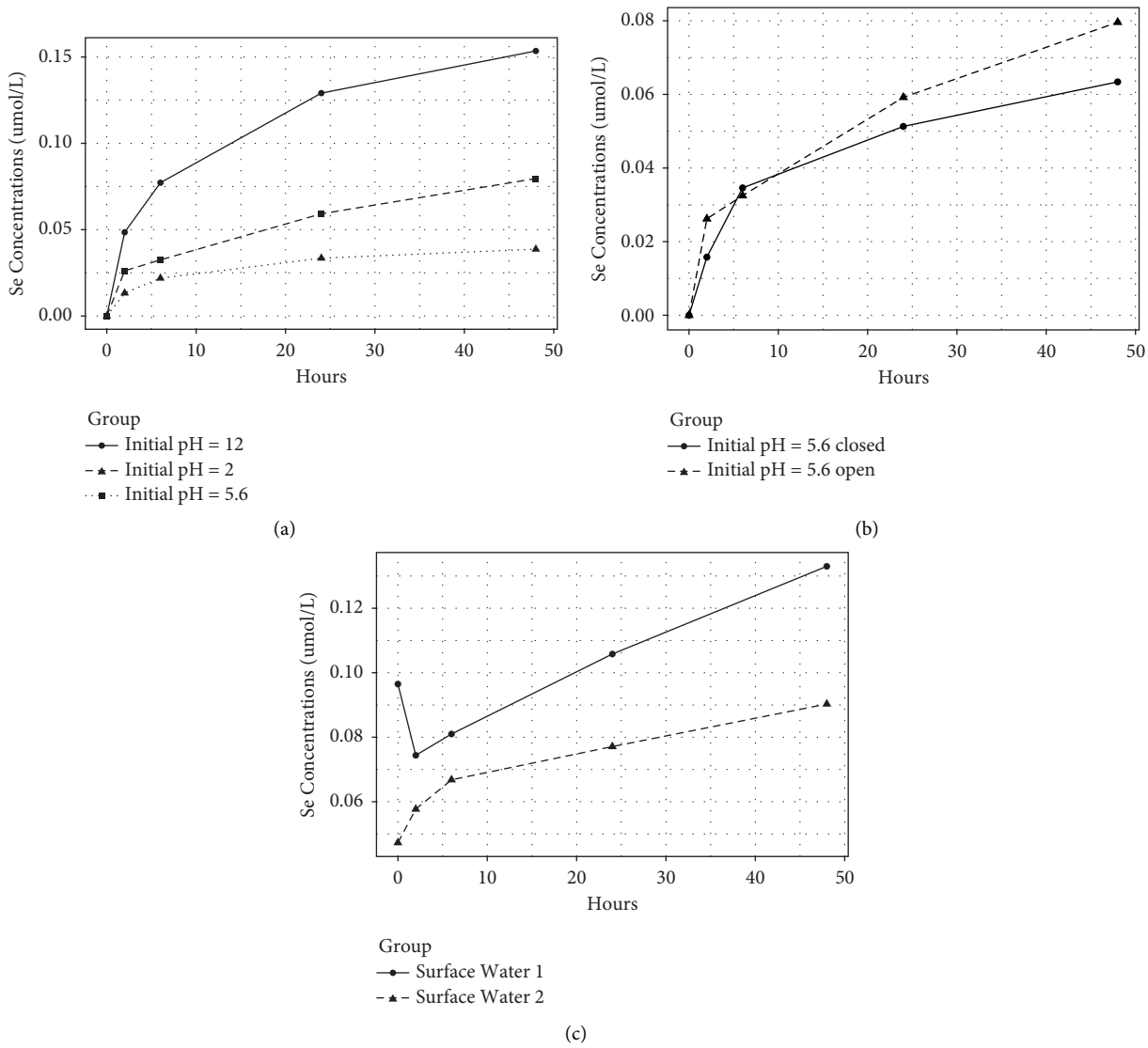

Figure 5: Results of experiments on selenium leaching. *Note.* This figure shows the results of experiments to study the behavior of selenium leaching, using 30 g of either coal seam host rock or coal samples, in 1000 g of solution. Three sets of leaching solutions were used. In (a), host rock samples were leached with high-purity water in an open-system arrangement with varying pH from an initial value of 2, to 5.6, and finally 12. In (b),the behavior of host rock samples being leached is compared with high-purity water at pH 5.6, under open- and closed-system conditions. In (c), leaching host rock samples are shown with two types of surface water under an open environment; the first surface water had an ionic strength of 24.6 mmol/L and sulfur content of 1.994 mmol/L, while the second had an ionic strength of 15.6 mmol/L and a sulfur content of 0.849 mmol/L.

absorption is nearly 100% up to pe 7, from that value onwards selenium is more likely to be released into solution, from 7 to 9 the selenium adsorption plummeted to negligible levels. These modeling results are like those obtained in the laboratory.

These pe modeling predicts what will happen to the selenium in the coal seam when mined. Before production, there is an anaerobic environment where pe values are low and selenium is likely to be absorbed into the coal seam. When the coal seam is open to air during mining, pe values will increase and the selenium adsorption will be reduced, thus selenium will be leached from the coal seam.

The selenium leached into the solution will adopt a variety of chemical forms—or chemical species—depending on the pH and pe values of the solution, as shown in Figure 4. This shows that at aerobic conditions, chemical species of Se^{+6} are more likely to form than Se^{+4}. The opposite will occur at anaerobic environments. This is relevant because the chemical form of a substance determines its absorption/mobility behavior as well as toxicity.

In this study, PHREEQC modeling results showed that SeO_3^{2-} has stronger adsorption ability than SeO_4^{2-}. At high pe values, the SeO_4^{2-}/total selenium ratio increases, indicating that the selenium adsorption is reduced. Similar results have been reported in literature; for example, Fernández-Martínez and Charlet [56] found the Se (VI) oxyanion selenate has little tendency to adsorb to solids or to precipitate out of solution compared to selenite Se (IV),

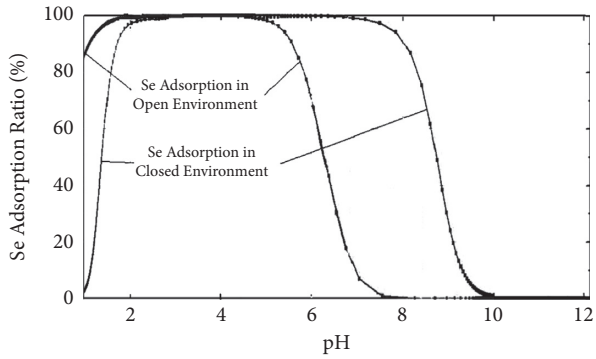

Figure 6: Modelling results of the ratio of selenium adsorption vs. pH solution. *Note.* This figure shows the modeling results of selenium adsorption and the effect of pH using the program PHREEQC version 2.15.05. For the simulation of selenium adsorption, it was assumed that there is the presence of 0.1 g ferrihydirte (HFO) in 1000 g of solution containing 0.6 nmol/L of selenium. The HFO surface area was considered to be 600 m^2/g, with $2.24e-3$ mol/g of weak sites and $5.6e-5$ mol/g of strong sites.

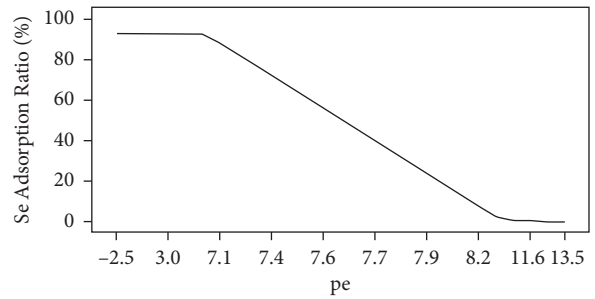

Figure 7: Modelling results of the ratio of selenium adsorption vs. pe. *Note.* This figure shows the modeling results of selenium adsorption and the effect of pe using the program PHREEQC version 2.15.05. For the simulation of selenium adsorption, the pH of the solution was kept at 7; the rest of assumptions were the same as those taken for the modeling of the effect of pH, described in Figure 6.

which has greater sorption affinity to metal oxyhydroxides, clays, and organic matter. Lopes et al. [57] found that Se sorption is mediated by its oxidation state, as selenite has more adsorption capacity than selenate, with the best affinity for metallic oxides and hydroxides mostly iron, manganese, and aluminum.

3.3.2. Competitive Adsorption. The effect of ionic strength on selenium leaching in coal seam was studied using two types of surface water samples, one of ionic strength 24.6 mmol/L and sulfur content of 1.994 mmol/L; and the other had ionic strength of 15.6 mmol/L and sulfur concentration of 0.849 mmol/L [58–62].

Results depicted in Figure 5(c) show that the [Se] in the solution obtained from the more concentrated surface water decreased during the first two hours of the experiment, increased slowly for four hours after that, to be increased promptly for the remaining time, reaching a concentration of 0.133 nmol/L after 48 h. In contrast, the [Se] in the solution got from the less concentrated surface water, increased steadily from beginning to end, reaching 0.0903 nmol/L after 48 h.

As seen, the effect of ionic strength on selenium leaching in host rock is better illustrated in the more concentrated solution, where a clear example of competitive adsorption is displayed. Such competition is likely to arise from sulfate and phosphate ions taking the place of selenium on adsorbent surfaces [32], such as clay minerals and HFO.

To study the effect of the dissolved ions on the adsorption of dissolved selenium, two "hypothetical" solutions were designed with major ions compositions similar either to coal mine water or surface water. The hypothetical coal mine water was modeled at both anaerobic and aerobic environments; while the surface water was modeled only considering that it was in contact with air. Under such conditions, for all cases, major ions were separately added and withdrawn from the hypothetical water in question to examine the major ions impact on the selenium adsorption, during these modeling experiments, the ionic strength was kept by addition of nonreactive ions such as nitrate. Modelling results showed that only dissolved sulfate reduced the selenium adsorption.

Figure 8 shows the effect that sulfur has on selenium adsorption. In the hypothetical coal mine water under anaerobic conditions, sulfur starts to compete when sulfur concentrations were above 4 and up to 12 mmol/L, reaching its highest interfering effect at around 8 mmol/L when selenium adsorption is reduced in almost 80%.

Once the dissolved major ions competing with selenium for adsorption was identified and its behavior was estimated; this study focused on identifying the selenium species most affected by sulfur at the existing conditions at the coal mines in Xuzhou district. As mentioned before and shown in Figure 7, pe is around 0 in the anaerobic environment and above 10 in the aerobic environment; as a result, Se^{+4} species will be more likely to form under the anaerobic environment, while Se^{+6} species will be more abundant under the aerobic environment. Thus, the adsorption of SeO_4^{2-} is quite likely to be reduced by the presence of sulfur under anaerobic conditions; in contrast to the adsorption of SeO_3^{2-} that is less impacted by the changing concentration of sulfur at aerobic conditions.

This study's results on the impact of sulfur on selenium adsorption could be explained by the fact that selenium and sulfur have similar structure and chemical character. Furthermore, similar findings have been reported previously; for example, You et al. [32] found that sulfate, phosphate, and carbonate reduced SeO_3^{2-} adsorption. They studied selenium adsorption on the layered double hydroxides (LDH) using 25 ml of solution containing 200 mg of LDH and 25 cmol/L of SeO_3^{2-}. When the $[SO_4^{2-}]/[SeO_3^{2-}]$ ratio was higher than 30, the selenium adsorption ratio reduced from 6 cmol/kg to about 1 cmol/kg.

Goh and Lym [30] also reported similar findings to those shown here; these authors studied the competitive adsorption of SO_4^{2-} on SeO_3^{2-} and SeO_4^{2-} and observed that the latter showed a significant decrease with increasing concentrations of SO_4^{2-}. In contrast, SeO_3^{2-} did not show a

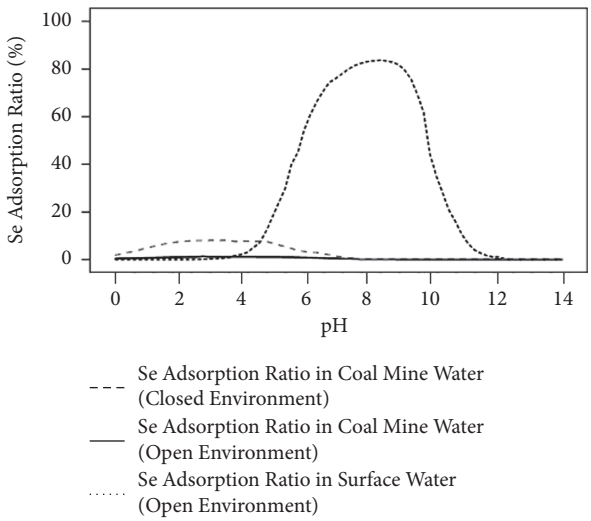

Figure 8: Modelling results of the ratio of selenium adsorption in two solutions with different ionic strengths. *Note.* This figure shows the modeling results of selenium adsorption and the effect of the concentration of dissolved major ions in two solutions using the program PHREEQC version 2.15.05. For the simulation of selenium adsorption, these two solutions were designed to represent the composition of surface and coal mine waters, with ionic strength of 68.3 and 24.6 mmol/L, respectively. The rest of assumptions were as described before.

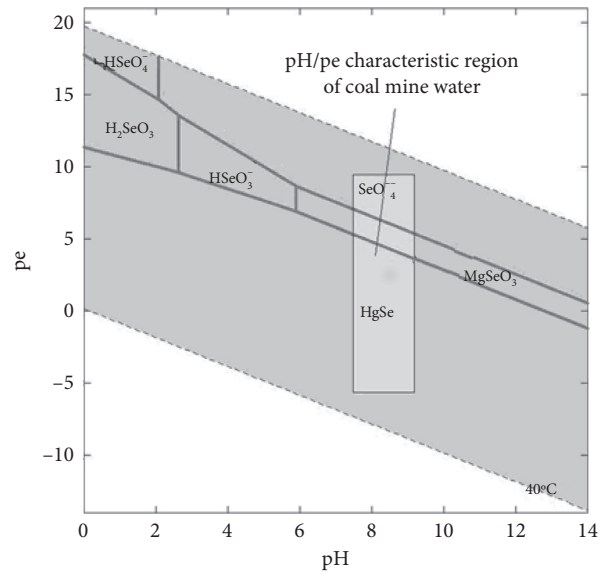

Figure 9: pH-pe diagram of selenium species in coal mine water in the Xuzhou-Datun coal mine district. *Note.* To prepare this diagram, the concentration of major and minor ions was set to match that of the coal mine water composition: SO_4^{2-}: 25.47 mmol/L; Cl^-: 14.1 mmol/L1; HCO_3^{2-}: 2.072 mmol/L; Na^+: 60.97 mmol/L; Ca^{2+}: 0.8148 mmol/L; Mg^{2+}: 1.699 mmol/L; Se: 0.6 nmol/L; Hg: 0.042 nmol/L; Pb: 0.25 nmol/L. Temperature was established to 40°C similar to the temperature in the coal mine.

significant impact. Previously mentioned authors [63–65] have adduced these differences could be explained if one considers that SeO_3^{2-} could be adsorbed on HFO surface by strong specific binding mechanism (inner-sphere complex), while SeO_4^{2-} may only form weak bonding on the HFO surface (outer-sphere complex) so it could be easily displaced by SO_4^{2-}. Mo et al. [66] reported that in divalent sulfate anions, Se (VI) sorption is almost completely inhibited at sulfate concentration close to 8.3 mmol/L.

3.4. Dissolved Selenium in the Xuzhou-Datun Coal Mine: A Hypothesis. Based on the analytical and modeling results, the high concentrations of selenium found in the Xuzhou-Datun coal mine water could be briefly explained as follows:

The selenium occurs in coal as clay minerals, and sulfide minerals in host rock. These minerals release selenium during the process of water-rock interaction. Accompanying the mining activity, pH and pe changes, then the release behavior may change either. In a closed environment, pyrite and other sulfide mineral is relatively stable. When the minerals open to air, pe value would rise, then the sulfide mineral reacted with water faster, so the selenium would be released to water. Clay minerals may transform from illite to kaolinite, then the selenium would be released.

In aerobic environments, higher pe and higher sulfur concentrations in water were found, which led to a high concentration of dissolved selenium in coal mine water. Thus, the oxidation and dissolution of selenium mineral and/or releasing from clays becomes the controlling impact on the selenium leaching. This explains why, despite that this coal mine district has coal seams with low concentrations of selenium, this element is in such high concentrations in the coal mine water. Moreover, dissolved selenium will be found in different chemical species that determine their mobility and adsorption.

In the Xuzhou-Datun coal mines, selenium-bearing minerals associated with coal seam are dominantly of a sulfidic type; however, selenium could also be in clay or organic form. All forms are unstable under aerobic environments.

In addition to pe, pH will have an important impact on selenium minerals dissolution and speciation of dissolved selenium species. Figure 9 shows the selenium pH-pe diagram in the coal mine water in Xuzhou-Datun coal mine district. Typical pH (7.5–9) and pe (3 to 12) values in coal mine water are marked by the gray area in the diagram. As seen, selenium can be dissolved as SeO_4^{2-} in aerobic environments for pe values above 7 or 8. With increasing pe in the coal mine water, the pyrites, and some selenium minerals such as magnesium selenate, tiemannite, and clausthalite will be oxidized and dissolved.

4. Conclusions

The concentration of selenium in the coal mine water from the Xuzhou-Datun Coal mines is high and poses a potential risk to pollute the surrounding surface water, though the selenium in coal and host rock is relatively low.

Leaching experiments carried out during this study showed that high values of pH, pe, and ionic strength enhanced selenium leaching in the coal mine water at the Xuzhou-Datun coal mine district. Adsorption and

dissolution processes in the solid phase controlled the behavior of such selenium leaching.

The selenium releasing mainly from sulfide minerals from host rock, and clay minerals from coal, respectively.

Modeling carried out in this study estimated that the main selenium species are weakly adsorbed at the typical conditions found in the Xuzhou-Datun coal mine environment. Such adsorption is impacted by pH, pe, and presence of dissolved major ion, especially sulfate. At acid pHs, the selenium adsorption on HFO is strong, and hence its leaching is limited; in contrast, at alkaline pHs, such adsorption is weak enhancing selenium leaching. The effect of alkaline pH will be increased if there is dissolved sulfur in the environment because sulfate will compete with selenium to be absorbed.

Oxidation and dissolution of selenium minerals may be the source of dissolved selenium in the coal mine water at the Xuzhou-Datun coal mine district. Pyrites, and some other selenium bearing minerals such as sphalerite, clausthalite, and tiemannite, may be the main selenium carriers in the coal seam; all of these are unstable at aerobic environments.

Data Availability

The datasets used and/or analyzed during the current study are available from the corresponding author on reasonable request.

Conflicts of Interest

The authors declare no conflicts of interest.

Acknowledgments

This study was supported by the https://doi.org/10.13039/501100012226Fundamental Research Funds for the Central Universities (No. 3142014005) and the https://doi.org/10.13039/501100017680Colleges and Universities in Hebei Province Science and Technology Research Project (No. ZD2016204). The testting of samples was carried out in the Jiangsu Provincial Coal Geology Research Institute, the Analysis and Test Center of the China University of Mining and Technology, the School of Geosciences of the Nanjing University and the Imperial College, London. The authors would like to thank all of them for their support.

References

[1] S. J. Hamilton, "Review of selenium toxicity in the aquatic food chain," *The Science of the Total Environment*, vol. 326, no. 1–3, pp. 1–31, 2004.

[2] U. Tinggi, "Essentiality and toxicity of selenium and its status in Australia: a review," *Toxicology Letters*, vol. 137, no. 1-2, pp. 103–110, 2003.

[3] Q. T. Dinh, Z. Cui, J. Huang et al., "Selenium distribution in the Chinese environment and its relationship with human health: a review," *Environment International*, vol. 112, pp. 294–309, 2018.

[4] H.-J. Sun, B. Rathinasabapathi, B. Wu, J. Luo, L.-P. Pu, and L. Q. Ma, "Arsenic and selenium toxicity and their interactive effects in humans," *Environment International*, vol. 69, pp. 148–158, 2014.

[5] J. B. Taylor, L. P. Reynolds, D. A. Redmer, and J. S. Caton, "Maternal and fetal tissue selenium loads in nulliparous ewes fed supranutritional and excessive selenium during mid- to late pregnancy," *Journal of Animal Science*, vol. 87, no. 5, pp. 1828–1834, 2009.

[6] X. Chen, G. Yang, J. Chen, X. Chen, Z. Wen, and K. Ge, "Studies on the relations of selenium and Keshan disease," *Biological Trace Element Research*, vol. 2, no. 2, pp. 91–107, 1980.

[7] K. Ge and G. Yang, "The epidemiology of selenium efficiency in the etiological study of endemic disease in China," *American Journal of Clinical Nutrition*, vol. 57, no. l, pp. 259–263, 1993.

[8] A. D. Lemly, "Selenium poisoning of fish by coal ash wastewater in Herrington Lake, Kentucky," *Ecotoxicology and Environmental Safety*, vol. 150, pp. 49–53, 2018.

[9] E. M. Chua, N. Flint, S. P. Wilson, and S. Vink, "Potential for biomonitoring metals and metalloids using fish condition and tissue analysis in an agricultural and coal mining region," *Chemosphere*, vol. 202, pp. 598–608, 2018.

[10] S. Huang, M. Hua, J. Feng et al., "Assessment of selenium pollution in agricultural soils in the Xuzhou district, northwest Jiangsu, China," *Journal of Environmental Sciences*, vol. 21, no. 4, pp. 481–487, 2009.

[11] H. R. El-Ramady, É. Domokos-Szabolcsy, T. A. Shalaby, J. Prokisch, and M. Fári, "Selenium in agriculture: water, air, soil, plants, food, animals and nanoselenium," in *CO_2 Sequestration, Biofuels and Depollution, Environmental Chemistry for a Sustainable World*, E. Lichtfouse, J. Schwarzbauer, and D. Robert, Eds., Springer International Publishing, Cham, Switzerland, pp. 153–232, 2015.

[12] A. Khamkhash, V. Srivastava, T. Ghosh, G. Akdogan, R. Ganguli, and S. Aggarwal, "Mining-related selenium contamination in Alaska, and the state of current knowledge," *Minerals*, vol. 7, no. 3, p. 46, 2017.

[13] R. B. Finkelman, C. A. Palmer, and P. Wang, "Quantification of the modes of occurrence of 42 elements in coal," *International Journal of Coal Geology*, vol. 185, pp. 138–160, 2018.

[14] C. C. Zhou, G. J. Liu, D. Wu, T. Fang, R. W. Wang, and X. Fan, "Mobility behavior and environmental implications of trace elements associated with coal gangue: a case study at the Huainan Coalfield in China," *Chemosphere*, vol. 95, pp. 193–199, 2014.

[15] I. Pumure, J. J. Renton, and R. B. Smart, "The interstitial location of selenium and arsenic in rocks associated with coal mining using ultrasound extractions and principal component analysis (PCA)," *Journal of Hazardous Materials*, vol. 198, pp. 151–158, 2011.

[16] Y. M. Nakamaru and J. Altansuvd, "Speciation and bioavailability of selenium and antimony in non-flooded and wetland soils: a review," *Chemosphere*, vol. 111, pp. 366–371, 2014.

[17] L. Winkel, B. Vriens, G. Jones, L. Schneider, E. Pilon-Smits, and G. Bañuelos, "Selenium cycling across soil-plant-atmosphere interfaces: a critical review," *Nutrients*, vol. 7, no. 6, pp. 4199–4239, 2015.

[18] K. Xing, S. Zhou, X. Wu et al., "Concentrations and characteristics of selenium in soil samples from Dashan Region, a selenium-enriched area in China," *Soil Science & Plant Nutrition*, vol. 61, no. 6, pp. 889–897, 2015.

[19] K. G. Bhattacharyya and S. S. Gupta, "Adsorption of a few heavy metals on natural and modified kaolinite and

montmorillonite: a review," *Advances in Colloid and Interface Science*, vol. 140, no. 2, pp. 114–131, 2008.

[20] C. B. Tabelin, T. Igarashi, M. Villacorte-Tabelin et al., "Arsenic, selenium, boron, lead, cadmium, copper, and zinc in naturally contaminated rocks: a review of their sources, modes of enrichment, mechanisms of release, and mitigation strategies," *The Science of the Total Environment*, vol. 645, pp. 1522–1553, 2018.

[21] G. Cornelis, C. A. Johnson, T. V. Gerven, and C. Vandecasteele, "Leaching mechanisms of oxyanionic metalloid and metal species in alkaline solid wastes: a review," *Applied Geochemistry*, vol. 23, no. 5, pp. 955–976, 2008.

[22] M. A. Palmer, E. S. Bernhardt, W. H. Schlesinger et al., "Mountaintop mining consequences," *Science*, vol. 327, no. 5962, pp. 148-149, 2010.

[23] A. Iwashita, Y. Sakaguchi, T. Nakajima, H. Takanashi, A. Ohki, and S. Kambara, "Leaching characteristics of boron and selenium for various coal fly ashes," *Fuel*, vol. 84, pp. 479–485, 2004.

[24] N. Jordan, C. Lomenech, N. Marmier, E. Giffaut, and J.-J. Ehrhardt, "Sorption of selenium(IV) onto magnetite in the presence of silicic acid," *Journal of Colloid and Interface Science*, vol. 329, no. 1, pp. 17–23, 2009.

[25] N. Jordan, A. Ritter, H. Foerstendorf et al., "Adsorption mechanism of selenium(VI) onto maghemite," *Geochimica et Cosmochimica Acta*, vol. 103, pp. 63–75, 2013.

[26] G. Zelmanov and R. Semiat, "Selenium removal from water and its recovery using iron (Fe^{3+}) oxide/hydroxide-based nanoparticles sol (NanoFe) as an adsorbent," *Separation and Purification Technology*, vol. 103, pp. 167–172, 2013.

[27] M. O. M. Sharrad, H. Liu, and M. Fan, "Evaluation of FeOOH performance on selenium reduction," *Separation and Purification Technology*, vol. 84, pp. 29–34, 2012.

[28] E. I. El-Shafey, "Removal of Se(IV) from aqueous solution using sulphuric acid-treated peanut shell," *Journal of Environmental Management*, vol. 84, no. 4, pp. 620–627, 2007.

[29] S.-L. Lo and T.-Y. Chen, "Adsorption of Se(IV) and Se(VI) on an iron-coated sand from water," *Chemosphere*, vol. 35, no. 5, pp. 919–930, 1997.

[30] K. H. Goh and T. T. Lim, "Geochemistry of inorganic arsenic and selenium in a tropical soil: effect of reaction time, pH, and competitive anions on arsenic and selenium adsorption," *Chemosphere*, vol. 55, pp. 849–859, 2003.

[31] G. E. Schwartz, N. Rivera, S.-W. Lee et al., "Leaching potential and redox transformations of arsenic and selenium in sediment microcosms with fly ash," *Applied Geochemistry*, vol. 67, pp. 177–185, 2016.

[32] Y. You, G. F. Vance, and H. Zhao, "Selenium adsorption on Mg-Al and Zn-Al layered double hydroxides," *Applied Clay Science*, vol. 20, no. 1-2, pp. 13–25, 2001.

[33] T. Su and J. Wang, "Modeling batch leaching behavior of arsenic and selenium from bituminous coal fly ashes," *Chemosphere*, vol. 85, no. 8, pp. 1368–1374, 2011.

[34] M. Totland, I. Jarvis, and K. E. Jarvis, "An assessment of dissolution techniques for the analysis of geological samples by plasma spectrometry," *Chemical Geology*, vol. 95, no. 1-2, pp. 35–62, 1992.

[35] P. J. Potts and P. Robinson, "Sample preparation of geological samples, soils and sediments," in *Sample Preparation for Trace Element Analysis*, Z. Mester and R. Sturgeon, Eds., Elsevier, Amsterdam, The Netherlands, pp. 723–763, 2003.

[36] C. Li, H. Liang, S. Wang, and J. Liu, "Study of harmful trace elements and rare earth elements in the Permian tectonically deformed coals from Lugou Mine, North China Coal Basin, China," *Journal of Geochemical Exploration*, vol. 190, pp. 10–25, 2018.

[37] M. W. Donner, B. Bicalho, C. Sinn, and W. Shotyk, "Selenium and sulphur in Athabasca bituminous sands mineral and bitumen fractions," *Fuel*, vol. 224, pp. 718–725, 2018.

[38] Y.-W. Chen, X. Yu, E. Appiah-Hagan et al., "Utilization of coal fly ash and drinking water sludge to remove anionic As(V), Cr(VI), Mo(VI) and Se(IV) from mine waters," *Journal of Environmental Chemical Engineering*, vol. 6, no. 2, pp. 2470–2479, 2018.

[39] W. Stumm and J. J. Morgan, *Aquatic Chemistry: Chemical Equilibria and Rates in Natural Waters*p. 155, Third edition, John Wiley & Sons, Hoboken, NJ, USA, 1996.

[40] D. A. Dzombak and F. M. M. Morel, *Surface Complexation Modeling: Hydrous Ferric Oxide*, John Wiley & Sons, New York, NY, USA, 1990.

[41] G. Cornelis, S. Poppe, T. Van Gerven, E. Van den Broeck, M. Ceulemans, and C. Vandecasteele, "Geochemical modelling of arsenic and selenium leaching in alkaline water treatment sludge from the production of non-ferrous metals," *Journal of Hazardous Materials*, vol. 159, no. 2-3, pp. 271–279, 2008.

[42] L. Q. Xu, "Environmental behavior of Se in Chinese environments," M.Sc. Thesis, Research Center for Eco-Environmental Sciences, Chinese Academy of Sciences, Beijing, China, 1988.

[43] R. N. White, J. V. Smith, D. A. Spears, M. L. Rivers, and S. R. Sutton, "Analysis of iron sulphides from UK coal by synchrotron radiation X-ray fluorescence," *Fuel*, vol. 68, no. 11, pp. 1480–1486, 1989.

[44] E. L. Zodrow and F. Goodarzi, "Environmental implications of elements associated with pyrite concentrates from coal in the sydney coalfield (upper carboniferous), Nova Scotia, Canada," *Energy Sources*, vol. 15, no. 4, pp. 639–652, 1993.

[45] C. A. Palmer, S. J. Mroczkowski, R. B. Finkelman, S. S. Crowley, and J. H. Bullock Jr, "The use of sequential leaching to quantify the modes of occurrence of elements in coal," in *Proceedings of the 15th Annual International Pittsburgh Coal Conference*, p. 28, Pittsburgh, PA, USA, 1998.

[46] L. Y. A. Kizilstein and O. A. Shokhina, "Geochemistry of selenium in coal: environmental aspect," *Geokhimiya [Geochemistry]*, vol. 4, pp. 434–440, 2001.

[47] R. B. Finkelman, "Modes of occurrence of trace elements in coal," Ph.D. Thesis, p. 329, Department Chemistry University of Maryland, College Park, MD, USA, Department Chemistry University of Maryland, 1980.

[48] J. C. Hower and J. D. Robertson, "Clausthalite in coal," *International Journal of Coal Geology*, vol. 53, pp. 221–225, 2003.

[49] A. Yahya and D. B. Johnson, "Bioleaching of pyrite at low pH and low redox potentials by novel mesophilic Gram-positive bacteria," *Hydrometallurgy*, vol. 63, pp. 181–188, 2001.

[50] G. A. Canty and J. W. Everett, "Alkaline injection technology: field demonstration," *Fuel*, vol. 85, pp. 17-18, 2006.

[51] C. Fan, H. Li, Q. Qin, S. He, and C. Zhong, "Geological conditions and exploration potential of shale gas reservoir in Wufeng and Longmaxi formation of southeastern Sichuan Basin, China," *Journal of Petroleum Science and Engineering*, vol. 191, Article ID 107138, 2020.

[52] S. Jiang, Y. Zuo, M. Yang, and R. Feng, "Reconstruction of the Cenozoic tectono-thermal history of the Dongpu Depression, Bohai Bay Basin, China: constraints from apatite fission track and vitrinite reflectance data," *Journal of Petroleum Science and Engineering*, vol. 205, Article ID 108809, 2021.

[53] B. Liu, R. Spiekermann, C. Zhao et al., "Evidence for the repeated occurrence of wildfires in an upper Pliocene lignite deposit from Yunnan, SW China," *International Journal of Coal Geology*, vol. 250, Article ID 103924, 2022.

[54] A. Li, M. Zhang, W. Ma, D. Li, and Y. Xu, "Sugar-disguised bullets for combating multidrug-resistant bacteria infections based on an oxygen vacancy-engineered glucose-functionalized MoO3-x photo-coordinated bienzyme," *Chemical Engineering Journal*, vol. 431, Article ID 133943, 2022.

[55] C. Zhan, Z. Dai, M. R. Soltanian, and X. Zhang, "Stage-wise stochastic deep learning inversion framework for subsurface sedimentary structure identification," *Geophysical Research Letters*, vol. 49, no. 1, 2022.

[56] A. Fernández-Martínez and L. Charlet, "Selenium environmental cycling and bioavailability: a structural chemist point of view," *Reviews in Environmental Science and Biotechnology*, vol. 8, Article ID 81e110, 2009.

[57] G. Lopes, F. W. Ávila, and L. R. G. Guilherme, "Selenium behavior in the soil environment and its implication for human health," *Ciencia E Agrotecnologia*, vol. 41, no. 6, pp. 605–615, 2017.

[58] X. Zhang, F. Ma, Z. Dai et al., "Radionuclide transport in multi-scale fractured rocks: a review," *Journal of Hazardous Materials*, vol. 424, Article ID 127550, 2022.

[59] X. Zhang, F. Ma, S. Yin et al., "Application of upscaling methods for fluid flow and mass transport in multi-scale heterogeneous media: a critical review," *Applied Energy*, vol. 303, Article ID 117603, 2021.

[60] Y. Liu, Z. Zhang, X. Liu, L. Wang, and X. Xia, "Ore image classification based on small deep learning model: evaluation and optimization of model depth, model structure and data size," *Minerals Engineering*, vol. 172, Article ID 107020, 2021.

[61] Y. Liu, Z. Zhang, X. Liu, L. Wang, and X. Xia, "Efficient image segmentation based on deep learning for mineral image classification," *Advanced Powder Technology*, vol. 32, no. 10, pp. 3885–3903, 2021.

[62] X. Chen, C. Huang, H. Wang, W. Wang, X. Ni, and Y. Li, "Negative emotion arousal and altruism promoting of online public stigmatization on COVID-19 pandemic," *Frontiers in Psychology*, vol. 12, Article ID 652140, 2021.

[63] P. C. Zhang and D. L. Sparks, "Kinetics and mechanisms of sulfate adsorption/desorption on goethite using pressure-jump relaxation," *Soil Science Society of America Journal*, vol. 54, no. 5, pp. 1266–1273, 1990.

[64] J. G. Catalano, Z. Zhang, P. Fenter, and M. J. Bedzyk, "Inner-sphere adsorption geometry of Se(IV) at the hematite (100)-water interface," *Journal of Colloid and Interface Science*, vol. 297, no. 2, pp. 665–671, 2006.

[65] J. Dong, R. Deng, Z. Quanying, J. Cai, Y. Ding, and M. Li, "Research on recognition of gas saturation in sandstone reservoir based on capture mode," *Applied Radiation and Isotopes*, vol. 178, Article ID 109939, 2021.

[66] Y. Mo, T. Vincent, C. Faur, and E. Guibal, "Se(VI) sorption from aqueous solution using alginate/polyethylenimine membranes: sorption performance and mechanism," *International Journal of Biological Macromolecules*, vol. 147, pp. 832–843, 2020.